

Compact Silicon Photonic Interleaver Using Loop-Mirror-Based Michelson-Gires-Tournois Interferometer

Xinhong Jiang, Jiayang Wu, Yuxing Yang, Ting Pan, Junming Mao,
Boyu Liu, Ruili Liu, Yong Zhang, Ciyuan Qiu, and Yikai Su

State Key Lab of Advanced Optical Communication Systems and Networks, Department of Electronic Engineering
Shanghai Jiao Tong University, Shanghai 200240, China
yikaisu@sjtu.edu.cn

Abstract: A compact ($125 \mu\text{m} \times 376 \mu\text{m}$) silicon photonic interleaver is proposed and experimentally demonstrated using loop-mirror-based Michelson-Gires-Tournois interferometer. The 3-dB and 20-dB bandwidths of the passband are $\sim 1.245 \text{ nm}$ and $\sim 1.709 \text{ nm}$, respectively.

OCIS codes: (130.3120) Integrated optics devices; (130.7408) Wavelength filtering devices

1. Introduction

Optical interleavers, which divide odd and even number of channels into two output ports, are key components in dense wavelength-division multiplexed (DWDM) systems [1]. Various schemes have been proposed to realize on-chip interleavers [2-6]. To achieve boxlike spectral response, ring-assisted Mach-Zehnder interferometer (MZI) structures are used to improve the roll-off of the interleavers [3-6]. However, these schemes exhibit large physical sizes since large radii of ring resonators are required to meet the demand of narrow channel spacing. In addition, a large length difference of the MZI arms equal to half of the ring circumference is needed to achieve a boxlike spectrum.

In this paper, to the best of our knowledge, we propose and experimentally demonstrate the first compact silicon photonic interleaver with boxlike spectral response implemented by loop-mirror-based Michelson-Gires-Tournois interferometer (MGTI), which takes advantages of reflective optical paths to reduce the footprint and improve the wavelength-tuning efficiency. As shown in Fig. 1(a) and (b), the Gires-Tournois etalons (GTEs) of the bulk MGTI [7] are replaced by cascaded loop mirrors [8]. The GTEs are utilized as phase-dispersive mirrors to ensure boxlike transmission passband [7]. Compared to travelling-wave resonators such as ring resonators, the cavity length ($d = l_1 + l_2$) of the standing-wave GTE is nearly half shorter [10]. Moreover, the required length difference ($\Delta L = l_4 - l_3$) of the MGTI arms is also half of the cavity length of the GTE due to double pass of the waveguides. Benefiting from the standing-wave characteristic of the GTE, the wavelength-tuning efficiency is twice higher than a travelling-wave resonator [10]. The designed device is monolithically integrated on a silicon-on-insulator (SOI) platform with a footprint of $125 \times 376 \mu\text{m}^2$. The free-spectral range (FSR) of the interleaver is $\sim 2.503 \text{ nm}$. The 3-dB and 20-dB bandwidths of the passband are $\sim 1.245 \text{ nm}$ and $\sim 1.709 \text{ nm}$, respectively, thus the 3-to-20 dB bandwidth ratio is $\sim 1:1.37$. By thermally tuning the length difference between the MGTI arms and the cavity lengths of the GTEs, the central wavelength can be effectively changed. In our experiment, the transmission spectrum is red shifted by $\sim 0.706 \text{ nm}$ with a heating power of 16.94 mW.

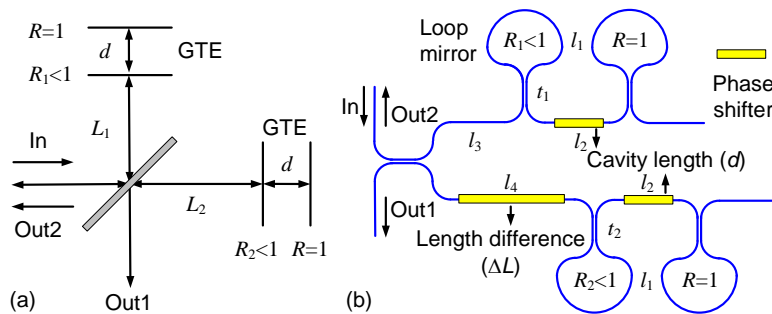


Fig. 1. (a) Bulk MGTI interleaver with two GTEs. (b) Schematic of the proposed interleaver. R denotes the reflectivity of the mirrors.

2. Device structure and operation principle

In Fig. 1(a), by replacing the GTEs of the bulk MGTI with cascaded loop mirrors, an on-chip interleaver is realized, as shown in Fig. 1(b). The total and partial reflection mirrors are realized by Sagnac-loop mirrors with 3-dB and non-3-dB directional couplers, respectively. In Fig. 1(b), $d = l_1 + l_2$ is the cavity length of the two GTEs. $\Delta L = l_4 - l_3$ is the length difference of the MGTI arms. The length difference ΔL is chosen to satisfy $\Delta L/d = 0.5$ for a boxlike spectral

response [9]. Based on transfer matrix method [11], the field transmissions of ports Out1 and Out2 can be given as follows:

$$\begin{aligned} t_{\text{Out1}} &= j(a_3^2 r_{\text{GTE1}} + a_4^2 r_{\text{GTE2}})/2 \\ t_{\text{Out2}} &= (a_3^2 r_{\text{GTE1}} - a_4^2 r_{\text{GTE2}})/2 \\ r_{\text{GTE}i} &= j(2a_1 t_i k_i + a_1^3 a_2^2 t_i k_i), i = 1, 2 \end{aligned} \quad (1)$$

where $r_{\text{GTE}i}$ ($i = 1, 2$) are the reflection functions of the two GTEs realized by two cascaded loop mirrors, respectively. t_i and k_i ($t_i^2 + k_i^2 = 1$, $i = 1, 2$) are the transmission and coupling coefficients of the non-3-dB directional couplers, respectively. $a_i = e^{-\alpha l_i - j\beta l_i}$ ($i = 1, 2, 3, 4$) are the transmission factors of the waveguides, with l_i ($i = 1, 2, 3, 4$) denoting the lengths of the waveguides, as shown in Fig. 1(b). α and $\beta = 2\pi n_g/\lambda$ are the loss factor and propagation constant of the silicon waveguides, respectively, with n_g denoting the group index of the transverse electric (TE) mode. In our simulations, the transmission coefficients t_1 and t_2 are chosen as 0.059 and 0.320, respectively. n_g is 4.35838 and α is 10.16 dB/cm.

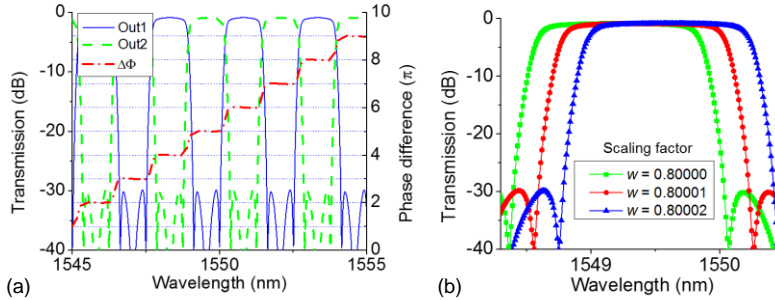


Fig. 2. (a) Transmission spectra of the interleaver, and phase difference of the MGTE arms at port Out1. (b) Central wavelength tuning from 1549.220 nm to 1549.270 nm.

Figure 2(a) depicts the simulated transmission spectra from port In to ports Out1 and Out2. The suppression ratio of the interleaver is ~ 30 dB. The 3-dB bandwidth is ~ 1.220 nm and the 20-dB bandwidth is ~ 1.500 nm, i.e., the 3-to-20 dB bandwidth ratio is $\sim 1:1.23$. These enable a high channel isolation of the proposed interleaver. The physical origin of the boxlike spectral response is the constructive interference of outputs of the two MGTE arms in the pass band, while destructive interference happens in the stop band [9]. The phase difference $\Delta\Phi$ of the MGTE arms at port Out1 is shown by the red-dash-dot curve in Fig. 2(a), which approaches $2n\pi$ (n is an integer) in the passband, and $(2n + 1)\pi$ in the stopband at port Out1, leading to a boxlike spectrum.

To investigate the tunability of the device, we conduct simulations of the transmission spectra at port Out1 based on Eq. (1). ΔL and d are weighted by a scaling factor w to tune the central wavelength, which is realized by tuning the phase shifters along l_2 and l_4 while $\Delta L/d$ is kept as 0.5. Figure 2(b) presents the spectra of wavelength tuning when Δw is on the order of 1×10^{-5} . The central wavelength is red shifted by 0.05 nm with w changing from 0.80000 to 0.80002. To obtain the desired bandwidth, the parameters of both ΔL and d can be further optimized.

3. Device fabrication and measured transmission spectra

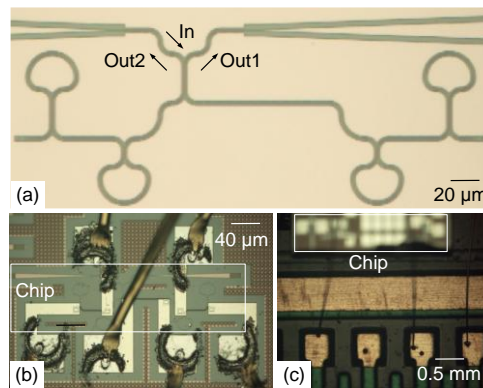


Fig. 3. Micrographs of (a) the fabricated chip, (b) the chip after wire-bonding, and (c) the chip on a PCB.

The designed device was fabricated on an 8-inch SOI wafer. A micrograph of the fabricated chip is shown in Fig. 3(a). The cross-sections of the waveguides are 450×220 nm². The footprint of the interleaver chip is 125×376 μm², which can be further reduced by using a folding layout [2]. TiN micro-heaters were fabricated along l_2 and l_4 to tune the

device. The metal pads connected to the heaters were wire-bonded to a printed circuit board (PCB) for electrical connections, as shown in Fig. 3(b) and (c).

A tunable continuous wave (CW) laser is used to scan the fabricated chip with a step size of 1 pm. Grating couplers for TE polarization are employed to couple light with single-mode fibers. The measured and fitted transmission spectra at port Out1 of the interleaver are shown in Fig. 4(a). The insertion loss of the chip is ~ 6 dB. A 12-dB coupling loss is introduced by a fiber coupling system. The measured suppression ratio of the interleaver is ~ 20 dB. The ripples in the stopband can be attributed to the non-ideal 3-dB directional couplers. The FSR of the spectrum is ~ 2.503 nm, which can be easily modified to fit the international telecommunications union (ITU) grids. The 3-dB bandwidth is ~ 1.245 nm and the 20-dB bandwidth is ~ 1.709 nm, which means a 3-to-20 dB bandwidth ratio of $\sim 1:1.37$. The fitting parameters include $t_1 = 0.279$, $t_2 = 0.470$, $n_g = 4.35838$, and $\alpha = 10.16$ dB/cm.

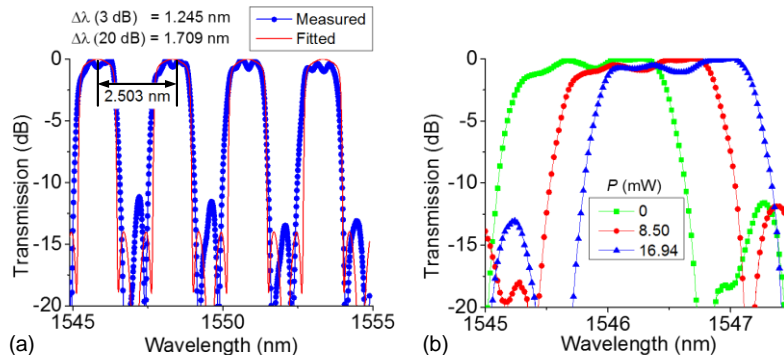


Fig. 4. (a) Measured and fitted transmission spectra. (b) Measured transmission spectra of central wavelength tuning.

The tuning of the central wavelength is also demonstrated. The heaters along l_2 and l_4 are used to tune the central wavelength, which redshifts as the effective cavity length increases. Figure 4(b) shows the measured transmission spectra of the device with different heating powers. The central wavelength is red shifted by ~ 0.706 nm with the heating power P ranging from 0 to 16.94 mW, corresponding to a wavelength-tuning efficiency of ~ 0.042 nm/mW, which can be further improved by optimizing the micro-heaters.

4. Conclusion

A compact tunable silicon photonic interleaver with a footprint of $125 \times 376 \mu\text{m}^2$ implemented by loop-mirror-based Michelson-Gires-Tournois interferometer is proposed and experimentally demonstrated. Compared to ring-based interleavers, the proposed device has a more compact footprint to achieve the same channel spacing due to the standing-wave characteristic of the GTEs and the double pass of the reflective optical paths. The FSR of the measured transmission spectrum is ~ 2.503 nm, which can be easily modified to fit the ITU grids. The 3-dB bandwidth is ~ 1.245 nm and the 20-dB bandwidth is ~ 1.709 nm, thus the 3-to-20 dB bandwidth ratio is $\sim 1:1.37$. By thermal tuning the device, a wavelength-tuning efficiency of ~ 0.042 nm/mW is achieved.

References

- [1] S. Cao *et al.*, "Interleaver technology: comparisons and applications requirements," *IEEE/OSA J. Light wave Technol.* **22**, 281-289 (2004).
- [2] T. Mizuno *et al.*, "12.5-GHz spacing compact and low-loss interleave filter using 1.5% Δ silica-based waveguide," *IEEE Photon. Technol. Lett.* **16**, 248-2486 (2004).
- [3] J. F. Song *et al.*, "Passive ring-assisted Mach-Zehnder interleaver on silicon-on-insulator," *Opt. Express* **16**, 8359-8365 (2008).
- [4] J. F. Song *et al.*, "Thermo-optical enhanced silicon wire interleavers," *IEEE Photon. Technol. Lett.* **20**, 2165-2167 (2008).
- [5] J. F. Song *et al.*, "Proposed silicon wire interleaver structure," *Opt. Express* **16**, 8359-8365 (2008).
- [6] L. W. Luo *et al.*, "High bandwidth on-chip silicon photonic interleaver," *Opt. Express* **18**, 23079-23087 (2010).
- [7] C. H. Hsieh *et al.*, "Flat-top Interleavers using two Gires-Tournois etalons as phase-dispersive mirrors in a Michelson interferometer," *IEEE Photon. Technol. Lett.* **15**, 242-244 (2003).
- [8] T. Zhang and Q. Sheng, "Interleaver design based on all-fiber G-T resonator formed by cascading two fiber loop mirrors," *Laser Journal* **25**, 41-42 (2005).
- [9] B. B. Dingel and M. Izutsu, "Multifunction optical filter with a Michelson-Gires-Tournois interferometer for wavelength-division-multiplexed network system applications," *Opt. Lett.* **23**, 1099-1101, (1998).
- [10] X. Sun *et al.*, "Tunable silicon Fabry-Perot comb filters formed by Sagnac loop mirrors," *Opt. Lett.* **38**, 567-569 (2013).
- [11] A. Yariv, "Critical coupling and its control in optical waveguide-ring resonator systems," *IEEE Photon. Technol. Lett.* **14**, 483-385 (2002).